



SUITABLE LOCATION OF SHEET PILE UNDER DAM RESTING ON SANDY SOIL WITH CAVITY

Laith J. Aziz¹ and Marwa H. Abdallah²

¹ Asst. Prof., Faculty of Engineering, University of Kufa, Email:
laith.aljarrah@uokufa.edu.iq

² MSc. Student, Faculty of Engineering, University of Kufa, Iraq. Email:
marrowa38@gmail.com

ABSTRACT.

This research describes the seepage characteristics of experimental model test of dam with cutoff located at different region (at dam heel, at mid floor of dam, and at dam toe). It is resting on sandy soil with cavity at different locations in X and Y directions (such as in Al-Najaf soil city). Thirty three model tests are performed in laboratory by using steel box to estimate the quantity of the seepage and flow lines direction. It was concluded that the best location of the cutoff wall is at the dam toe for model test with cavity ($\frac{X_c}{B} = 0$ and 0.5), but for model test with cavity ($\frac{X_c}{B} \geq 1$), the best location of the sheet pile wall becomes at the dam heel. For negative location of the cavity, the best location of the sheet pile wall is at the middle of the floor dam.

KEYWORDS: Quantity of seepage; Sheet pile; Cavity; Flow line

1. INTRODUCTION

Hydraulic structures are a specific type of engineering structures designed and executed in such a way in order to utilize it to control natural water or save industrial sources to ensure optimum use of water. One of the main causes of hydraulic structures failure is the seepage under the foundation. The seepage flow exerts pressure on the structure and generates erosive forces. In other words, the soil particles are moved under the hydraulic structure and in the water flow direction and this phenomenon call a piping.

Many methods have been developed for analyzing the seepage under dam and around sheet pile wall like empirical solution, numerical and experimental solution:

[Ghaly et. al. \(1991\)](#) studied the behavior of a model with a single sheet pile. The sheet pile was penetrated the thick sand and subjected to seepage flow to allow preparation of flooded sand to reach to the steady state flow. It was founded that the uplift behavior of the sheet pile and seepage quantity depended on sand properties.

[Abbas Z. \(1994\)](#) studied the conformal analysis of seepage below a hydraulic structure with an inclined cutoff. Conformal mapping techniques are used to obtain an exact solution for seepage flow below a hydraulic structure founded on permeable soil of infinite depth for a flat floor with an inclined cut-off at the downstream end. The exit gradient decreases considerably along a distance beyond the floor end with an increase in cut-off inclination.

[Al delewy et. al. \(2006\)](#) studied the optimum design of control devices for safe seepage under hydraulic structures. The finite-element method is used to analyze seepage through porous media below hydraulic structures with blanket, cut- off, or filter trench as seepage control devices. The effect of length and location of the control devices is investigated.

[Alsenousi and Mohamed \(2008\)](#) examined the effect of the changing the characteristics of soil foundation with inclined sheet pile wall on the values of the quantity of the seepage under the hydraulic structures. It may be inferred that the values of the exit gradient decreases with the increase in sheet pile inclination.

[Obead \(2013\)](#) used a finite element model to analyze the two- dimensional steady state seepage of water through the foundation of dam structure in the presence of inclined sheet pile as seepage control device. The uplift pressure head is decreased when the inclination of the sheet pile is towards the downstream part of the dam.

Shayan and Tokaldany (2014) studied the effects of upstream blanket and sheet pile on reducing seepage flow, exit gradient, and uplift force. It is observed that the best location of sheet pile to reduce seepage flow is at the downstream end.

Musa (2014) studied the influence of cavities on seepage under sheet pile wall for hydraulic structure embedded into cohesionless soil of Al-Najaf city with cavity. Depending on the tests results of the model with various size of the cavity, it shows that the quantity ratio (amount of discharge) and steady time decrease with the increase in the size of the cavity.

Al suhaili and Karim (2014) explain the optimal dimensions of small hydraulic structure cutoffs using coupled genetic algorithm and ANN Model. genetic algorithm model coupled with artificial neural network model was developed to find the optimal values of upstream, downstream cutoff lengths, length of floor and length of downstream protection required for a hydraulic structure. These were obtained for a given maximum difference head, depth of impervious layer and degree of anisotropy.

Hassan (2015) studied the application of a genetic algorithm for the optimization of a cutoff wall under hydraulic structures. A genetic algorithm (GA) model coupled with finite element modeling was developed here to find the optimal values of inclination angle and cutoff location for a hydraulic structure of a given cutoff depth to floor length ratio. The objective function to be minimized is the exit gradient function. The main constraint models are those that satisfy a factor of safety against uplift pressure which correspond with minimum floor thickness.

Taeh (2015) explained an experimental study of seepage and uplift pressure under hydraulic structures by physical model. The analysis of these experiments results of the models represented that the quantity of seepage, uplift pressure generated underneath the base of hydraulic structure, exist gradient at downstream side changes with different location and inclination of sheet pile.

Farhadian and Katibeh (2015) used the analytical methods and Digital Elevation Model and Site Groundwater Rating method to estimation the ground water seepage into Amirkabir tunnel for different sections through this tunnel. The obtained results were presented as a comparison between the different sections along the tunnel by using a mentioned method of the Site Groundwater Rating.

1.1. CAVITY PROBLEM

AL-Najaf , holy city, is located in the middle part of Iraq. The area of Al-Najaf city topography was contained on the limestone lays into underground surface as subsurface bedding. In Al-

Najaf soil, the limestone rock and the gypsum are within in the sedimentary deposits with the continuous ground water movement, the limestone rock and gypsum dissolve and generates many cavities at different locations (depths or horizontal location below ground surface level) and different shapes and sizes (AL-Ata'a, 2006) [2].

However, in the field of AL-Najaf soil, there are two types of cavity problems can be observed. In the first, a cavity exists initially into the soil mass (such as artificial cavity) due to the vault (oldest) building and then the water flow applied. In the second, there is initially no cavity in to the soil mass (natural cavity), but after the application of the water flow, the cavity will form into the soil mass (gypsum dissolve) as shown in Fig. 1.

Limestone layer is a carbonate rock composed largely of the mineral calcite. Natural underground water contains carbonic acid, which reacts with calcite to form calcium bicarbonate, a soluble substance that is carried away in solution. Calcium bicarbonate is approximately 30 times more soluble in water than calcium carbonate; for that reason, the carbonation reaction causes increasingly rapid dissolution of the limestone (Stokes et al., 1978).



Fig. 1. Different sizes of cavities into soil profile at AL-Najaf City.

1.2. AIMS OF RESEARCH

Studying the changing in the magnitudes of the quantity of the seepage under the dam when the soil mass contains cavity at different locations, recorded the time to reach condition of steady state flow, and drawing the flow lines directions through the soil and cavity.

2. PREPARATION OF MODEL

For all model tests, the soil used are prepared by mixing dry soil (buring from site) with water in percent corresponding to optimum water content, then spreading the soil inside the middle compartment of the box in six layers. Each layer is compacted to a unit weight equal to the

maximum dry unit weight ($\gamma_d=16.7\text{KN/m}^3$). The compaction process was selected to produce homogeneous sample that could be used for a parametric study in a laboratory testing program. The final dimensions of this homogeneous sample are ($H=300\text{ mm}$) in height, ($W=100\text{ mm}$) in width and ($L=500\text{ mm}$) in length. The cavities were prepared by placing PVC tube at a certain location. Following these, the placement of the sheet pile then compaction continued till the final level of the bed of the soil (ground surface level).

3. DESCRIPTION OF LABORATORY TESTING PROGRAM

The schematic diagram of the test preparation, water flowing, model cavity, model dam and sheet pile shown in Fig. 2. The difference in water levels between each side of dam are kept constant during test period. The seepage takes place under the dam, through soil and cavity. The water in upstream zone was maintained at a constant level by using a continuous supply of water from the upstream reservoir. The out wardness water from downstream is collected in a jar to measure the quantity of seepage with time. The test is stopped when flow becomes in steady state (the volume of water still constant with time).

The test procedure consists of three groups; the first was location of sheet pile at upstream side under the dam, the second group when the sheet pile located at mid-width of the dam, and the last the sheet pile located at downstream side under the dam. Each group consists of 11 tests one of these with no cavity and others with single cavity with different horizontal location defined by X_c -locations and different vertical location defined by Y_c -location. The descriptions of these parameters are listed in Table 1.

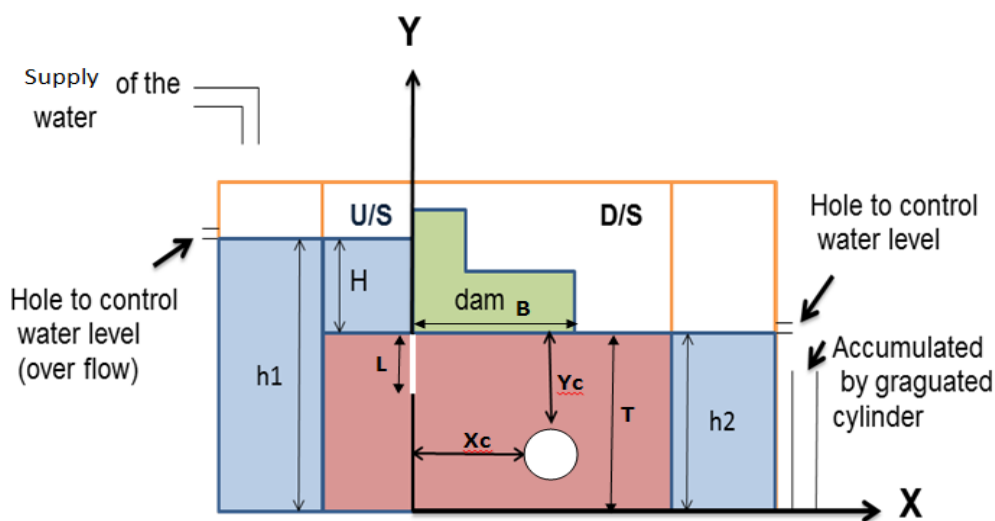


Fig. 2. Schematic of Dam – Soil – Cavity System Analyzed.

4. DRAWING FLOW LINES

In order to draw the flow lines at steady state flow for all model tests, the indicator color method was used to clear the flow lines of the seepage flow under the dam as shown in a typical curves of onice model test, Fig. 3.



Fig. 3. Typical flow lines pattern for model $\frac{b}{B} = 0$ with cavity $\frac{y_c}{T} = 0.5$ and $\frac{x_c}{B} = -0.74$.

5. THE EQUATION OF FLOW THROUGH A POROUS MEDIUM

5.1. Darcy's Law

The flow of water beneath the ground surface through all soils except coarse gravel and larger materials occurs as laminar flow (Harr 1962):

$$Re = \frac{VD\rho}{\mu} \leq 1 \dots\dots\dots(1)$$

Where

Re: Reynolds number.

V: Discharge velocity.(cm/sec)

D: Average of diameter of soil particles.(cm)

ρ : Density of fluid.(gm/cm³)

μ :Coefficient of viscosity.(gm/cm.sec)

For this condition, Darcy's law for water traveling through soils can be applied to determine the rate of quantity of flow as sited by (Carthy, 1982):

$$V_s = k i \dots\dots\dots(2)$$

Table 1. Tests program.

Test Number	$\frac{b}{B}$	$\frac{X_c}{B}$	$\frac{Y_c}{T}$
1 (No Cavity)	0	----	----
2	0	-0.74	0.5
3	0	0	0.5
4	0	0	0.75
5	0	0.5	0.25
6	0	0.5	0.5
7	0	0.5	0.75
8	0	1	0.25
9	0	1	0.5
10	0	1	0.75
11	0	1.74	0.5
12 (No Cavity)	0.5
13	0.5	-0.74	0.5
14	0.5	0	0.25
15	0.5	0	0.5
16	0.5	0	0.75
17	0.5	0.5	0.5
18	0.5	0.5	0.75
19	0.5	1	0.25
20	0.5	1	0.5
21	0.5	1	0.75
22	0.5	1.74	0.5
23 (No Cavity)	1
24	1	-0.74	0.5
25	1	0	0.25
26	1	0	0.5
27	1	0	0.75
28	1	0.5	0.25
29	1	0.5	0.5
30	1	0.5	0.75
31	1	1	0.5
32	1	1	0.75
33	1	1.74	0.5

Where:

V^s : Velocity through porous media.

k: Hydraulic conductivity.

i : Hydraulic gradient = $\frac{-dh}{dl}$.

h: Piezometrichead.

l : Distance along the flow line.

5.2. Laplace's Equation

The components of seepage flow through porous media according to the generalized form of Darcy's law are (Craig, 2004):

$$v_x = k_x \frac{\partial h}{\partial x} \dots \dots \dots (3)$$

$$v_y = k_y \frac{\partial h}{\partial y} \dots \dots \dots (4)$$

$$v_z = k_z \frac{\partial h}{\partial z} \dots \dots \dots (5)$$

Where:

v_x, v_y, v_z : Velocity components in the x, y, and z-direction, respectively.

k_x, k_y, k_z : hydraulic conductivity in the x, y, and z-direction, respectively.

Continuity is ensured by requiring that the net volume of water flowing per unit of time into or out of an element of soil be equal to the change per unit of time of the volume of water in that element as cited by (Terzaghi, 1996), For the steady state seepage condition , in which the change per unit of time of the volume of water in the element is zero, thus:

$$\frac{\partial v_x}{\partial x} + \frac{\partial v_y}{\partial y} + \frac{\partial v_z}{\partial z} = 0 \dots \dots \dots (6)$$

Where:

$$v_x = k_x \frac{\partial h}{\partial x}, v_y = k_y \frac{\partial h}{\partial y}$$

and $v_z = k_z \frac{\partial h}{\partial z}$

Equation (6) becomes

$$k_x \frac{\partial^2 h}{\partial x^2} + k_y \frac{\partial^2 h}{\partial y^2} + k_z \frac{\partial^2 h}{\partial z^2} = 0 \dots \dots \dots (7)$$

For the analysis of seepage, flow is considered to be two-dimensional and the equation is used in the form:

$$k_x \frac{\partial^2 h}{\partial x^2} + k_z \frac{\partial^2 h}{\partial z^2} = 0 \dots \dots \dots (8)$$

For isotropic soil, the permeability is independent of the direction of the flow $k_x = k_z$, the continuity equation in term of the velocity potential $\phi = k h$ is:-

$$\frac{\partial^2 \phi}{\partial x^2} + \frac{\partial^2 \phi}{\partial z^2} = 0 \dots \dots \dots (9)$$

This expression, known as Laplace's equation, describes the variation of hydraulic head in two-dimensional flow of the water through soil.

6. BOUNDARY CONDITIONS

The soil that used for analysis a seepage must be a defined parameters such as boundaries and permeability of the soil (Kareem, 2008). Before starting with the solution, boundaries conditions should be allocated at the steady state of a confined flow, the first type of the boundary conditions is reservoir boundary which are called equipotential lines. Where the piezometric head allocation along the reservoir boundaries is constant; that is:

$$H = H_o = \frac{p}{\gamma_w} + z \dots \dots \dots (10)$$

The second boundaries called impervious boundaries; the fluid can neither penetrate the boundary nor leave gaps, so the velocity component that normal to this boundary (V_n), must be zero ($\frac{\partial H}{\partial n} = 0$). Fig. 4 shown the Boundary conditions.

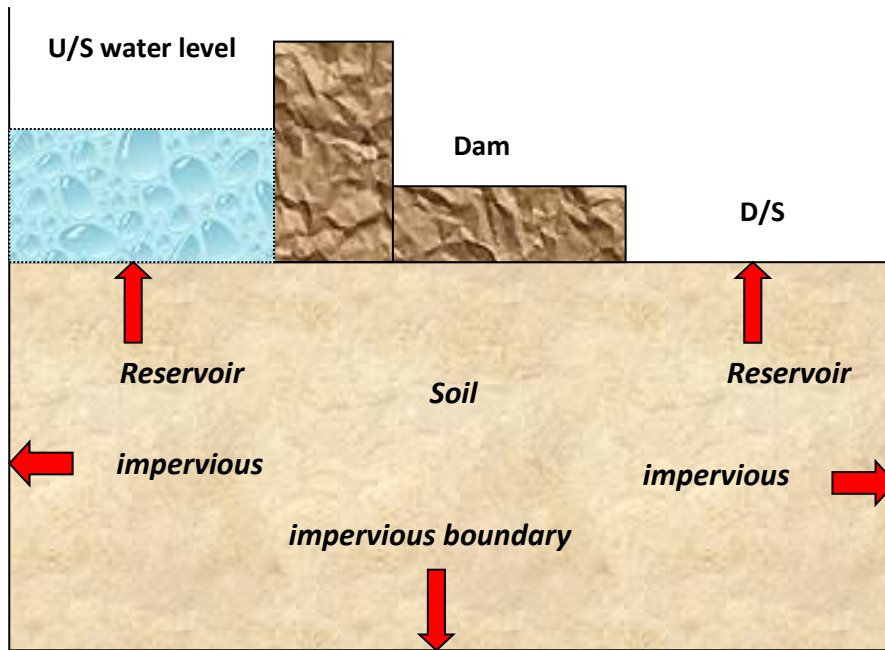


Fig. 4. Boundary conditions of seepage under a hydraulic structure.

7. FINITE ELEMENT

The finite element method is a very powerful numerical method. It requires the use of digital computer because of the large number of computations involved. In ground water flow problems, one could imagine that a region is subdivided into small elements, these elements may be two, or three dimensional and joined to each other by nodes existing on the element boundaries. Such that for each element the flow is described in terms of the head in the nodal points, and that then a system of equations is obtained from the conditions that the flow must be continuous at each node as cited by (El-Katib, 2009).

The field variable model describing an approximate variation of piezometric head (H_e) within the element is :

$$H^e(x, y) = \sum_{i=1}^n N_i(x, y) H_i \dots\dots\dots (11)$$

where:

x and y = The coordinates of element.

H_i = Nodal value of head, H, of element.

n = Number of nodes per element.

N_i = Shape function of the element.

and in matrix form

$$H^e = [N_i] \{H_i\} \dots\dots\dots(12)$$

Where:

H_i = The vector of nodal heads.

N_i = The matrix of shape functions.

The approximate solution of head distribution, H, throughout the flow domain is:

$$H = \sum_{e=1}^m [N_i] \{H_i\} \dots\dots\dots (13)$$

where:

m = The total number of elements in the flow domain.

The finite element method have two kind of elements (linear triangular element) and (quadrilateral quadratic element) in order to analyze the seepage problems through a porous medium.

In order to apply the finite element procedures, the model of the problem, should be presented in a numerical form. A typical description of the problem can containscalar parameters (number of nodes, elements),material properties, coordinates of nodal points, connectivity array for the finite elements and array of element types. This model is written under a package program titled as (Slide). Slide program can be used to model confined and unconfined flow situations.

8. RESULTS VALIDATION

Analytical methods based on the equations of water inflow into tunnels with respect to parameters such as permeability, water table, and tunnel (cavity) radius which it is comparison with present work results as shown in [Table 2](#).

Table 2. Values of the quantity of the seepage.

Item	Reference	The quantity of seepage (cm ³ /min)/cm	Equation	Description
1	Heuer (1995)	5.8	$Q = \frac{2\pi k H_0}{\ln(\frac{2Z}{r})} * 1/8$	Heuer reduction coefficient (1/8), r : radius flow, Z : depth of the tunnel, H_0 : hydraulic head, and k : equivalent permeability
2	Present work	5.6	From model test when the sheet pile located at the heel of dam with cavity at $(\frac{X_c}{B} = -0.74 \text{ and } \frac{Y_c}{T} = 0.5)$	-----
3	Freeze and Cherry (1979)	3.3	$Q = \frac{2\pi k H_0}{\ln(\frac{2H_0}{r})}$	r : radius flow, H_0 : hydraulic head, and k : equivalent permeability

From Table 2 can be noted that only small differences are found between the results of the experimental study with analytical equations [(Heuer (1995); and Freeze and Cherry (1979)].

9. DISCUSSION OF THE RESULTS

All tests have similar geometry with regards to sheet pile width, cavity diameter, thickness of flow region, the water heads at upstream and downstream, and embedment depth of the sheet pile. The laboratory test presented with an assumption of plane-strain condition.

To evaluate the effects of the sheet pile cutoff wall locations and the cavity locations on the seepage characteristics, using the results of laboratory model, as a results in terms the dimensionless parameters, also to facilitate comparison between the model test.

9.1. Model tests at shallow cavity depth with ($\frac{Y_c}{T}=0.25$) and ($\frac{X_c}{B}=0, 0.5$ and 1)

The influence for sheet pile location on the discharge ratio ($\frac{q}{q_0}$) for the cavity model tests located at fixed vertical location ($\frac{Y_c}{T} = 0.25$) and at a different horizontal locations ($\frac{X_c}{B} = 0, 0.5$ and 1) in steady state flow condition can be noted in Fig. 5. The value of ($\frac{q}{q_0}$) rapidly

increase when the sheet pile wall location moves from the dam heel toward the center line of the dam for ($\frac{X_c}{B} = 1$), but when the cavity located at ($\frac{X_c}{B} = 0$ and 0.5), the value of ($\frac{q}{q_0}$) decrease when the sheet pile location moves from the dam heel toward the dam toe.

The relationship between sheet pile location with the time ratio ($\frac{t}{t_0}$) for six model tests with cavity at fixed vertical location ($\frac{Y_c}{T} = 0.25$) and different horizontal location ($\frac{X_c}{B} = 0, 0.5$ and 1) at steady state flow condition indicates in Fig. 6. For model tests with cavity located at ($\frac{X_c}{B} = 1$), the value of ($\frac{t}{t_0}$) slightly decrease with moving the location of sheet pile ($\frac{b}{B}$) from the dam heel to the dam center line. But this behavior is inversed for model tests with cavity ($\frac{X_c}{B} = 0$ and 0.5).

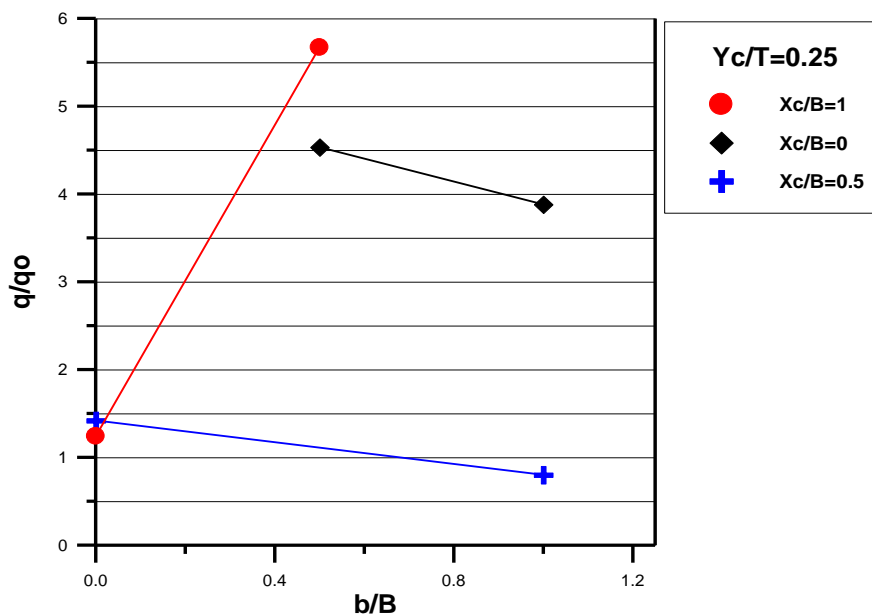


Fig. 5. The relationship between location of sheet pile with discharge ratio.

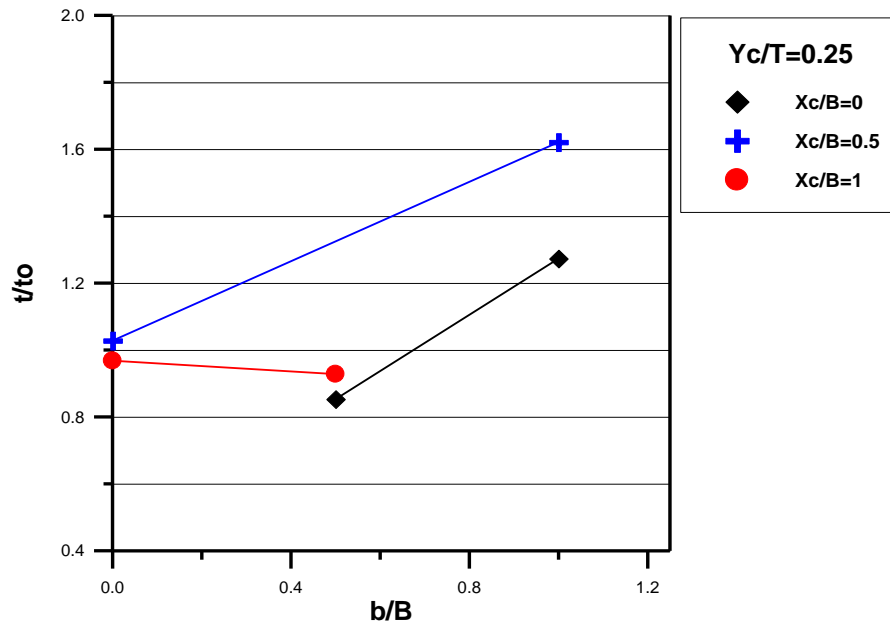


Fig. 6. The location of sheet pile versus time ratio.

9.2. Model tests with ($\frac{Y_c}{T}=0.5$) and ($\frac{X_c}{B}=-0.74, 0, 0.5, 1$ and 1.74)

A plot of the ratio of seepage discharge between cavity and no cavity ($\frac{q}{q_0}$) versus the sheet pile position ($\frac{b}{B}$) at different horizontal location ($\frac{X_c}{B}$) and at a certain cavity depth ($\frac{Y_c}{T} = 0.5$) is shown in Fig. 7. The curves of all models are convex downstream. The peak values of ($\frac{q}{q_0}$) when the sheet pile positioned under the center line of the floor dam for all model tests except for only model test with ($\frac{X_c}{B} = -0.74$). The values of ($\frac{q}{q_0}$) for model test with ($\frac{X_c}{B} = 0, 1$ and 1.74) are approximately equally at any location of the sheet pile. In other words, when the sheet pile located out the region of the dam, the ($\frac{q}{q_0}$) are equally. The model test with ($\frac{X_c}{B} = -0.74$) have a low values of ($\frac{q}{q_0}$) at sheet pile location (0 and 0.5), but it becomes a peak value when the sheet pile located at the dam toe.

Fig. 8 represents the location of sheet pile versus the time ratio ($\frac{t}{t_0}$) for model tests with cavity at fixed cavity depth ($\frac{Y_c}{T} = 0.5$) and different horizontal location ($\frac{X_c}{B} = -0.74, 0, 0.5, 1$ and 1.74) in steady state flow condition. It can be seen that for all model tests the value of ($\frac{t}{t_0}$) increase gradually with moving the sheet pile wall from the dam center to the dam toe. Also, the figure shows, the values of ($\frac{t}{t_0}$) of the ($\frac{b}{B} = 0$) and ($\frac{b}{B} = 0.5$) are approximately equal. For sheet pile positioned at the dam toe, the values of ($\frac{t}{t_0}$) of the model tests ($\frac{X_c}{B} =$

0, 1 and 1.74) (model tests located out the region of the dam) are larger values from that for other model tests.

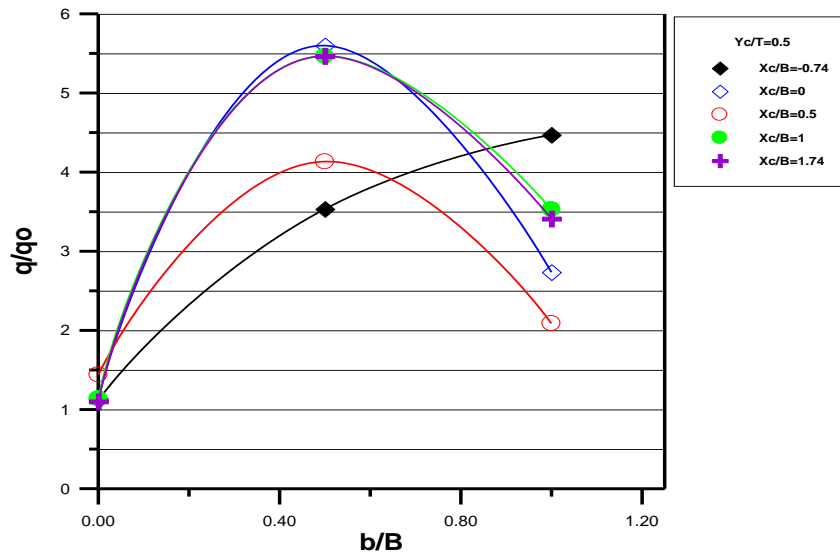


Fig. 7. The relationship between location of sheet pile with discharge ratio.

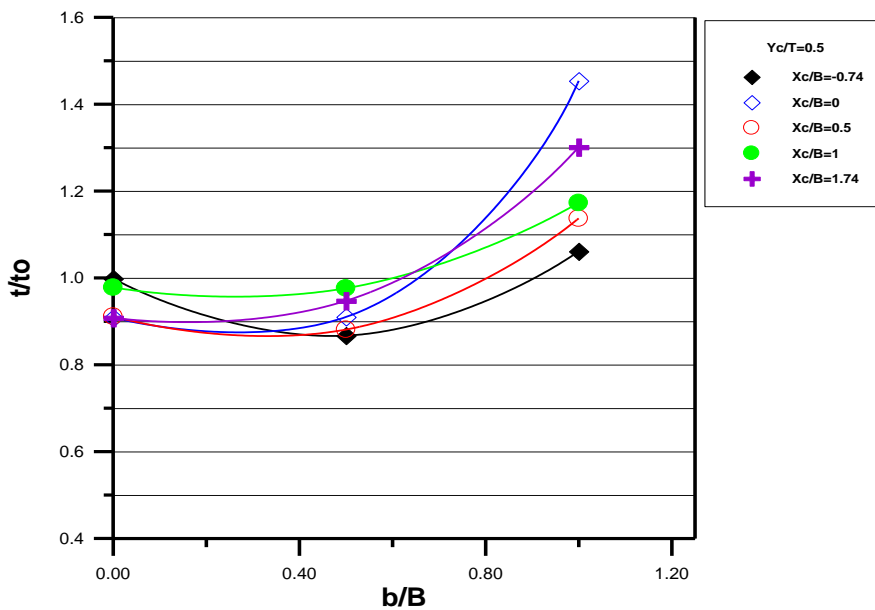


Fig. 8. The location of sheet pile versus time ratio.

9.3. Model tests with cavity deep ($\frac{Y_c}{T} = 0.75$) and ($\frac{X_c}{B} = 0, 0.5$ and 1)

Fig. 9 illustrates the effect of sheet pile location on discharge ratio ($\frac{q}{q_0}$) at steady state flow condition when the model tests with cavity at fixed vertical location ratio ($\frac{Y_c}{T} = 0.75$) and different horizontal location ratio ($\frac{X_c}{B} = 0, 0.5$ and 1). The values of ($\frac{q}{q_0}$) increase when the sheet pile location change from upstream toward the center of the dam width, after this point it decrease at location of sheet pile at downstream of the dam for all model tests. These curves of

the figure are similar to model tests of cavity with ($\frac{Y_c}{T} = 0.5$). The maximum values of the ($\frac{q}{q_0}$) with ($\frac{b}{B}$) can be observed for the model test with ($\frac{X_c}{B} = 1$). At model test with ($\frac{X_c}{B} = 0.5$), the values of ($\frac{q}{q_0}$) are minimum.

The values of the ratio ($\frac{t}{t_0}$) for all model tests ($\frac{X_c}{B} = 0, 0.5, \text{ and } 1$) decrease gradually when the sheet pile location moves from the dam heel to the dam center, after that it becomes rapidly increase when the sheet pile location change to the dam toe as shown in Fig. 10. At sheet pile positioned in the dam center, the values of ($\frac{t}{t_0}$) for model test ($\frac{X_c}{B} = 0$ and 0.5) are equal.

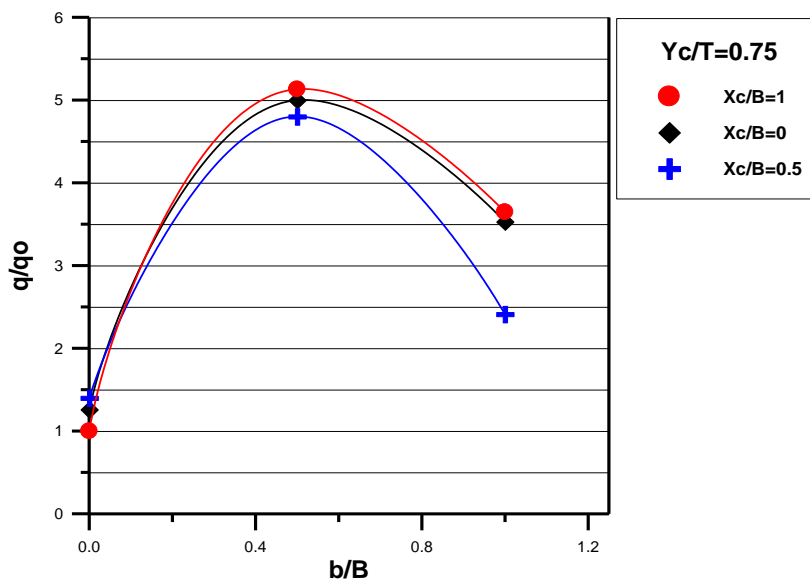


Fig. 9. The relationship between location of sheet pile with discharge ratio.

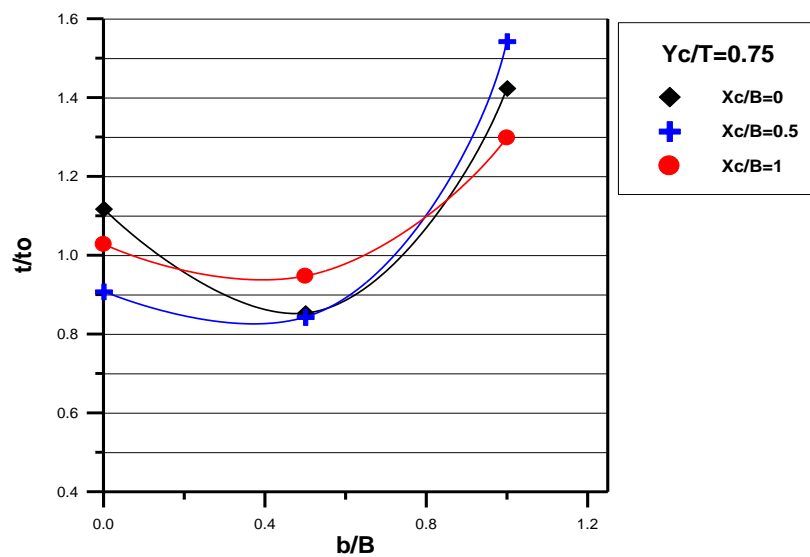


Fig. 10. The location of sheet pile versus time ratio.

9.4. Dam Performance

The performance of the dam is analyzed in terms of the quantity of seepage under the dam for cavity to no cavity condition ($\frac{q}{q_0}$) and also in terms of the time to reach the discharge to steady state case ($\frac{t}{t_0}$) for cavity to no cavity condition. Fig. 11 to 12 shows a well accepted correlation between predicted and observed ($\frac{q}{q_0}$) and ($\frac{t}{t_0}$). The mathematical representation of the family of the curves in previous section is represented by the following equation resulted from a regression analysis by Ms-Statistica.

$$\frac{q}{q_0} = C1 \left(\frac{b}{B}\right) \times \left(\frac{X_c}{B}\right)^2 + C2 \left(\frac{Y_c}{T}\right) \times \left(\frac{b}{B}\right)^2 + C3 \left(\frac{X_c}{B}\right) + (C4)b/B + \left(\frac{b}{B}\right)^2 / \left(\frac{Y_c}{T}\right) + C5 \left(\frac{Y_c}{T}\right)^2 + (C6 \left(\frac{b}{B}\right)^2)^5 + C7 \left(\left(\frac{Y_c}{T}\right) + \left(\frac{X_c}{B}\right)\right) C8 + (\exp(C9 \left(\frac{X_c}{B}\right) / (2 + C10)) / \left(\frac{X_c}{B}\right) + \left(\frac{Y_c}{T}\right)) + C11 \left(\left(\frac{X_c}{B}\right) + \left(\frac{Y_c}{T}\right)\right)^2 + C12 \left(2 + \left(\frac{X_c}{B}\right)\right)^2 + C13 \dots\dots\dots(14)$$

- | | | | | |
|----------|----------|-------------|-----------|-------------|
| C1=0.56 | C4=9.24 | C7=558.03 | C10=0.35 | C13=-553.53 |
| C2=6.84 | C5=-4.23 | C8=0.008 | C11=0.004 | |
| C3=-0.96 | C6=-1.66 | C9=-1845.81 | C12=-0.53 | |

$$\frac{t}{t_0} = C1 \left(\frac{X_c}{B}\right)^2 + C2 \left(\frac{Y_c}{T}\right)^2 \times \left(\frac{b}{B}\right)^2 + C3 \left(\frac{X_c}{B}\right) \times \left(\frac{b}{B}\right)^2 + C4 \left(\frac{b}{B}\right) + C5 \left(\frac{b}{B}\right)^2 \times \left(\frac{Y_c}{T}\right) + C6 \left(\frac{Y_c}{T}\right)^2 \times \left(\left(\frac{b}{B}\right) + 2\right) + (C7 + \left(\frac{Y_c}{T}\right))^{20} + C8 \left(\left(\frac{Y_c}{T}\right) \times \left(\frac{X_c}{B}\right)\right) + C9 \left(\left(\frac{Y_c}{T}\right) + \left(\frac{b}{B}\right)\right)^5 + C10 \left(\left(\frac{b}{B}\right)^2 \times \left(\frac{X_c}{B}\right)\right)^2 + C11 \left(\left(\frac{Y_c}{T}\right) \times \left(\frac{X_c}{B}\right) \times \left(\frac{b}{B}\right)\right)^{20} + C12 \left(\left(\frac{b}{B}\right) + \left(\frac{X_c}{B}\right)\right)^2 + C13 \left(\left(\frac{X_c}{B}\right)^2 + \left(\frac{Y_c}{T}\right)^2\right) C14 + C15 \left(8 + \left(\frac{b}{B}\right)^5\right)^3 + C16 \left(\frac{X_c}{B}\right) + C17 \dots\dots\dots(15)$$

- | | | | | |
|----------|----------|-----------|-----------|------------|
| C1=0.087 | C5=-2.72 | C9=-0.106 | C13=88.83 | C17=-88.98 |
| C2=6.63 | C6=-1.26 | C10=-0.57 | C14=0.005 | |
| C3=0.37 | C7=0.21 | C11=16.84 | C15=0.004 | |
| C4=0.102 | C8=1.4 | C12=0.023 | C16=-1.64 | |

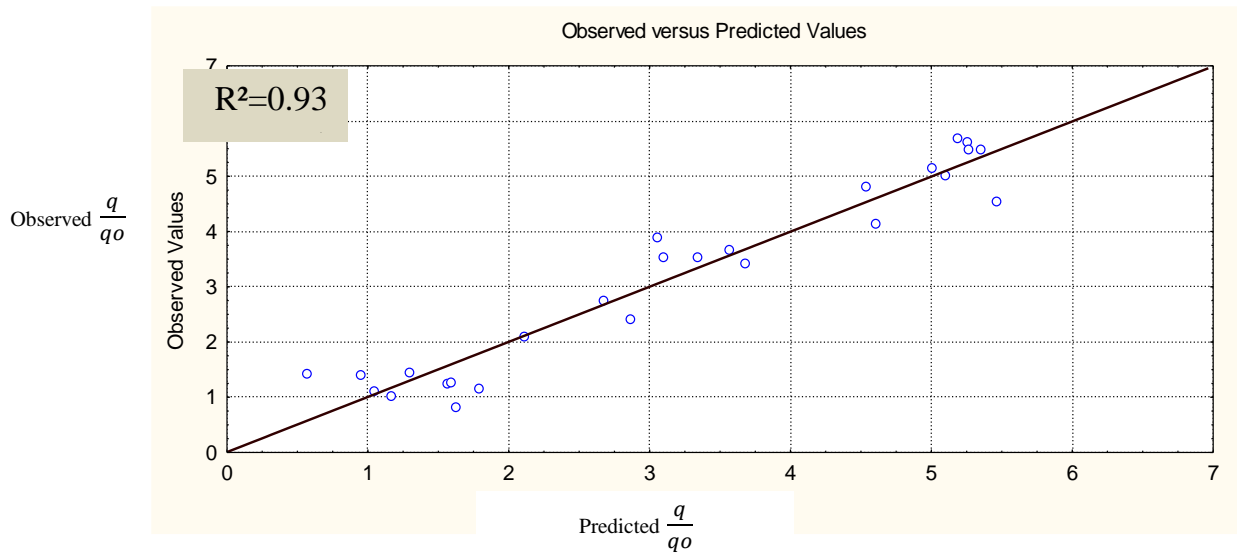


Fig. 11. Comparison of formula (14) with experimental results.

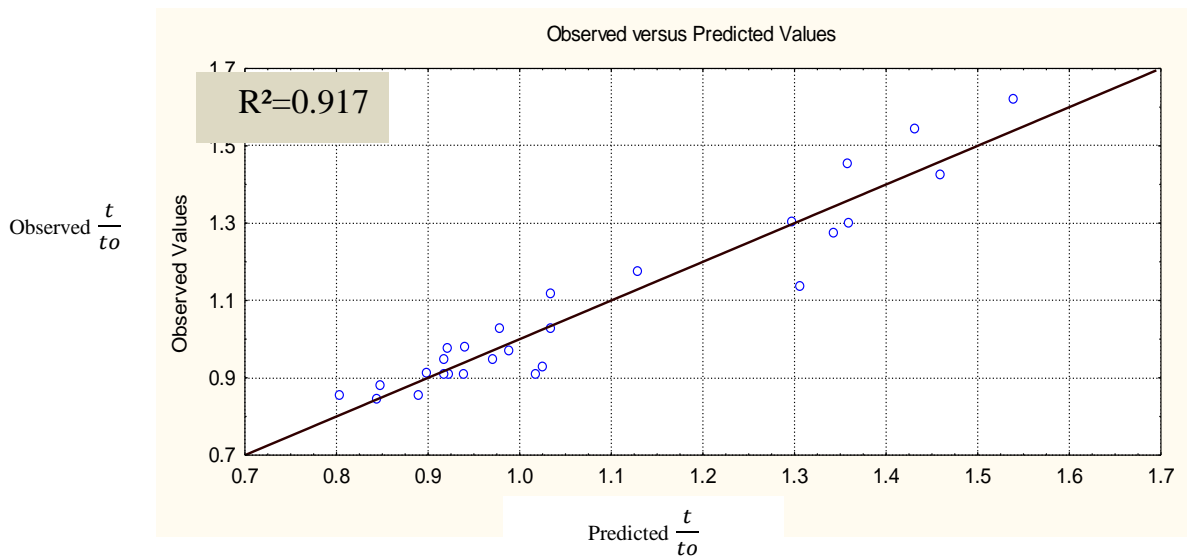


Fig. 12. Comparison of formula (15) with experimental results.

10. CONCLUSION

1. For all model tests in experimental work, the values of the seepage discharge under the hydraulic structure are changed with time, either increase or decrease until to reach the constant values at steady state flow.
2. When the cavity and sheet pile wall are located at the center line of the dam, the values of the quantity of the seepage are equally at the range of time from (500 to 650) min for model test with ($\frac{Y_c}{T} = 0.5$ and 0.75).

3. The values of the discharge seepage with time are convergent for model test with ($\frac{Y_c}{T} = 0.25$ and 0.5) when the sheet pile wall located at the center line of the dam with horizontal location of the cavity at the dam toe.
4. During the water flow period, the values of the seepage discharge for model test at cavity depth ($\frac{Y_c}{T} = 0.5$ and 0.75) are convergent when the sheet pile wall and the cavity are located at the dam toe.
5. Different flow lines mode (trend) can be observed for each model tests depending upon the geometry of the problem (location of cavity and sheet pile wall under the dam).
6. The effect of the cavity depth ($\frac{Y_c}{T}$) on the time ratio ($\frac{t}{t_0}$) is very small when the sheet pile wall located at the dam center line or when the sheet pile wall located at the dam heel.
7. For all model tests, the values of the seepage flow for the cavity conditions are greater than that of no cavity condition, but this behavior is opposite for only one model test with cavity at location ($\frac{X_c}{B} = 0.5$ and $\frac{Y_c}{T} = 0.25$).
8. Empirical equations (1) and (2) can be used to estimate the quantity of the seepage, water flow time for cavity conditions at a different locations and for sheet pile wall at located in the heel or middle floor or toe of the dam.
9. At any cavity depth case ($\frac{Y_c}{T}$), the minimum values of the seepage flow can be observed in cavity with ($\frac{X_c}{B} = 0.5$) when the sheet pile wall is located at the toe or at the middle floor of the dam.
10. When the sheet pile wall located at the downstream side or at the center line of the dam, the values of the quantity of the seepage are equally for model tests with cavity at location ($\frac{X_c}{B} \geq 1$ and $\frac{Y_c}{T} = 0.5$).

11. REFERENCES

- Abbas, Z. (1994), "Conformal analysis of seepage below a hydraulic structure with an inclined cutoff", *International Journal for Numerical and Analytical Methods in Geomechanics*, Volume 18, Issue 5.
- AL-Ata'a, M. J. (2006), "Earth of Najaf: History, Geological heritage and Natural Wealth", Najaf, Iraq.
- Al delewy, A. A. (2006), "Optimum Design of Control Devices for Safe Seepage under Hydraulic Structures", *Journal of Engineering and Development*, Vol. 10, No.1, March (2006) ISSN 1813-7822.
- Alsenousi; KH.F., and Mohamed; H.G. (2008), "Effect of Inclined Cutoff and Soil Foundation Characteristics on Seepage Beneath Hydraulic Structure", Twelfth International Water Technology Conference, IWTC12, Alexandria, Egypt.
- Al suhaili, R. H. and Karim, R. A. (2014), "Optimal Dimensions of Small Hydraulic Structure Cutoffs Using Coupled Genetic Algorithm and ANN Model", ISSN: 17264073 Year: 2014 Volume: 20 Issue: 2 Pages: 1-19 Publisher: Baghdad University.
- Carthy, D.F., (1982), "Essentials of Soil Mechanics and Foundations", New Jersey-Prentice Hall.
- Ghaly, A. Hanna, A. and Hanna, M. (1991). "Uplift Behavior of Screw Anchors in Sand", *J.Getech. Eng., ASCE*, Vol.(117), No.(5), P.794-808.
- Craig, R. F. (2004), "Craig's Soil Mechanics", Seventh edition, Taylor & Francis e-Library.
- El-Jumaily, K.K. and Al-Bakry, H.M. (2013), "Seepage analysis through and under hydraulic structures applying finite volume method", www.pdfactory.com.
- El-Katib, A. A. (2009), "Analysis of Seepage Beneath Water Retaining Structures Founded on Spatially Random Soil", MS.C Thesis, University of Babylon, Iraq.
- Farhadian, H.; and Katibeh, H., (2015), "Groundwater Seepage Estimation into Amirkabir Tunnel Using Analytical Methods and DEM and SGR Method", *International Journal of Civil, Environmental, Structural, Construction and Architectural Engineering* Vol:9, No: 3.
- Freeze; R.A., Cherry;J.A. (1979), "Groundwater", Prentice-Hall, Englewood Cliffs, New Jersey
- Harr, A.E., (1962), "Ground Water and Seepage", Mc Graw-Hill Book Company.

Hassan, W. H. (2015), "Application of a genetic algorithm for the optimization of a cutoff wall under hydraulic structures", *Journal of Applied Water Engineering and Research*, Volume 5, 2017- Issue1.

Heuer; R.E. (1995), "Estimating rock-tunnel water inflow", In *Proceeding of the Rapid Excavation and Tunneling Conference*. Ed. G. E, Williamson and I. M. Growring; pp. 41-60.

Kareem, H. H., (2008), "Stability of Concrete Gravity Dams with Intermediate Filter", M.Sc. Thesis in water Resources Engineering, University of Babylon.

Musa, T. A. (2014), "Influence of Cavities on Seepage under Sheet Pile Wall for Hydraulic Structures", MS.C Thesis, University of Kufa, Iraq.

Obead; I.H. (2013), "Effect of Position and Inclination Angle of Cutoff Wall on Seepage Control in the Foundation of Dam Structure", *Journal of Kerbala University*, Vol. 11, No. 4 Scientific.

Stokes, W.L., S. Judson, S. and M.D. Picard. (1978), "Introduction to Geology", Englewood Cliffs, NJ: Prentice-Hall, Inc.

Shayan; H.K., and Tokaldany; E.A. (2014), "Effects of blanket, drains, and cutoff wall on reducing uplift pressure, seepage, and exit gradient under hydraulic structure", *International Journal of Civil Engineering* Vol. 13, No.4A,(amiri@ut.ac.ir)

Taeh, H. K. (2015), "Experimental Study of Seepage and Uplift Pressure under Hydraulic Structures by Physical Model", MS.C Thesis, University of Babylon, Iraq.

Terzaghi, K., Peck, R. B. and Mesri, G. (1996), "Soil Mechanics in Engineering Practice", New York, Wiley.